Elsevier Editorial System(tm) for International Conference on Metallurgical Coatings and Thin Films
Manuscript Draft

Manuscript Number:

Title: Electrochemical Boriding of Molybdenum in Molten Borax

Article Type: Full Length Article

Section/Category: Symposia F and G

Keywords: Boriding; molybdenum; molten salt electrolysis; Mo2B4.027; Mo2B5

Corresponding Author: Dr. Ozgenur Kahvecioglu, Ph.D.

Corresponding Author's Institution: Istanbul Technical University

First Author: Ozgenur Kahvecioglu, Ph.D.

Order of Authors: Ozgenur Kahvecioglu, Ph.D.; Vivekanand Sista, PhD; Osman L Eryilmaz, PhD; Ali Erdemir, PhD; Servet Timur, PhD

Abstract: In this study, molybdenum plates (99.5% purity) were subjected to electrochemical boriding in a molten borax electrolyte in order to synthesize molybdenum boride phases on exposed surfaces. Electrochemical boriding was carried out at temperatures of 900, 950, and 1000°C for a duration of 30-180 min at a current density of 0.5 A/cm2. Cross-sectional microscopic examination of the plates indicated formation of 20- to 50-μm thick boride layers, depending on process temperature and duration. These layers consisted of two distinct boride phases: Mo2B4.027 and Mo2B5. The boride-layer cross-sectional hardness was in the range of 1900-3250 HV with 50 g load. The adhesion of the boride coating to the molybdenum substrate was determined by a Rockwell C indentation adhesion test machine. The boride layers produced due to the electrochemical boriding technique were thick, hard, dense, and homogeneous.

Suggested Reviewers: Hasan Erdem Camurlu PhD
Asst. Prof. Dr., Mechanical Engineering, Akdeniz University
ecamurlu@akdeniz.edu.tr
Dr. Camurlu studied the preparation of single phase molybdenum boride.

Yu Ligen PhD
Research fellow, School of Mechanical & Aerospace Engineering, Nanyang Technological University
mlgyu@ntu.edu.sg
Dr. Ligen worked on pack boriding of molybdenum asisted with spark plasma sintering.

Jaap C. Schouten PhD.
Prof. Dr., Chemical Engineering and Chemistry, Eindhoven University of Technology
j.c.schouten@tue.nl
Dr. Schouten is an expert on protective coatings synthesized in molten salts. He is also studying the oxidation behavior of the coatings.

C L Yeh PhD

Department of Mechanical and Automation Engineering, Da-Yeh University
clyeh@mail.dyu.edu.tw
Dr. Yeh worked on the preparation of molybdenum borides by combustion synthesis.

**MANUSCRIPT REPORT FORM**

**PAPER NUMBER (if known):** 489

**TITLE OF PAPER:** Electrochemical Boriding of Molybdenum in Molten Borax

**CORRESPONDING AUTHOR:** Ozgenur Kahvecioglu

**FULL MAILING ADDRESS:** Istanbul Technical University, Department of Metallurgy and Materials Engineering, Room: A-201, 34469, Maslak, Istanbul, Turkey

**TELEPHONE:** + 90(212) 285 7366

**FAX:** + 90(212) 285 3427

**E-MAIL:** kahveciog3@itu.edu.tr
ozgenur78@gmail.com

# AUTHOR'S CERTIFICATION

**This is to certify that I have obtained the necessary authorization for publication of the enclosed paper #489 (Electrochemical Boriding of Molybdenum in Molten Borax) in the Proceedings of the ICMCTF 2012 Conference and in *Surface and Coatings Technology/Thin Solid Films* and that the paper is original and unpublished and is not being considered for publication elsewhere.**

**Corresponding Author**

**Ozgenur Kahvecioglu**

**Istanbul Technical University**

## Highlights

- Electrochemical boriding has been performed to form very hard, dense and homogeneous boride layers on molybdenum.
- Increasing process duration and temperature resulted in thicker boride layers.
- Boron-rich boride phases were produced on molybdenum surface.
- $Mo_2B_{4.027}$ phase was obtained as the predominant phase on top of the borided surface and reported for the first time in this study.
- The activation energy obtained by electrochemical boriding was found to be 47.6 kJ/mol.

*Manuscript

# Electrochemical Boriding of Molybdenum in Molten Borax

O. Kahvecioglu[a,*], V. Sista[b], O.L. Eryilmaz[b], A. Erdemir[b], S. Timur[a]

[a] Istanbul Technical University, Department of Metallurgy and Materials Engineering, Istanbul, Turkey

[b] Argonne National Laboratory, Energy Systems Division, Argonne, IL, U.S.A

## Abstract

In this study, molybdenum plates (99.5% purity) were subjected to electrochemical boriding in a molten borax electrolyte in order to synthesize molybdenum boride phases on exposed surfaces. Electrochemical boriding was carried out at temperatures of 900, 950, and 1000°C for a duration of 30-180 min at a current density of 0.5 A/cm$^2$. Cross-sectional microscopic examination of the plates indicated formation of 20- to 50-µm thick boride layers, depending on process temperature and duration. These layers consisted of two distinct boride phases: $Mo_2B_{4.027}$ and $Mo_2B_5$. The boride-layer cross-sectional hardness was in the range of 1900–3250 HV with 50 g load. The adhesion of the boride coating to the molybdenum substrate was determined by a Rockwell C indentation adhesion test machine. The boride layers produced due to the electrochemical boriding technique were thick, hard, dense, and homogeneous.

**Keywords:** Boriding, molybdenum, molten salt electrolysis, $Mo_2B_{4.027}$, $Mo_2B_5$

## 1. Introduction

Borides of VIB group metals have been an attractive research area in terms of their unique physical and physicochemical properties, including high melting points, high hardness values, excellent oxidation resistance, high electrical and thermal conductivities at elevated temperature, high chemical stability toward acidic media, excellent catalytic properties, and excellent resistance to both mechanical and corrosive wear [1-13]. Consequently, their borides find uses in several industrial and high-temperature structural applications. In particular, due to its high thermal conductivity, molybdenum is used for high temperature applications to assist rapid heat transfer from the reaction zone (i.e., in secondary gas-phase screening reactors) to the environment [3,13]. Galvanic molybdenum coatings are known to be highly corrosion resistant while they can also increase wear (especially erosion-cavitation wear [14]) and abrasion resistance as well as the surface hardness of different materials [15]. Additionally, this coating enhances the performance of engineering components such as pistons, rings, and shafts [16]. However, molybdenum fails to retain its corrosion resistance when in contact with hot aggressive gases and water vapor at high temperatures [3,14]. At this point, a protective coating of a boride layer would alleviate such deficiencies under harsh operating conditions.

Synthesis of molybdenum borides has been explored in the past by various means, such as pack boriding [7,17], spark plasma sintering [7], solid-state reaction [8], self-propagating high-temperature synthesis [18], mechanochemical synthesis [4,19], volume combustion synthesis [20], multiphase reaction diffusion in a salt bath [3], and electrochemical boriding [3,13,21-22]. Of these, electrochemical boriding in molten salts appeared to give the most desirable forms of boride layers in the shortest duration.

Industrial applications of molybdenum borides include use as hard coatings in machine tools, high-performance gear parts, and golf shoe spikes [5]. Specific uses of molybdenum borides differ in terms of intrinsic properties of each boride compound. For example, $Mo_2B_5$ has excellent catalytical properties and, hence, finds application as an electrode in fuel cells that rely on an acidic electrolyte [10]. This boride is also used for reinforcing $MoSi_2$ because of its good electrical and thermal conductivity ($\lambda$ = 50 W/m•K, [13]) and relatively high coefficients of thermal expansion ($\alpha = 8.6 – 9.9 \times 10^{-6}$/K) [23]. Due to its high electrical conductivity, $MoB_x$ (x = 1.0–2.0) is being used as a conductive barrier layer between aluminum conductor and silicon substrate at contact points in semiconductor devices [24]. Furthermore, MoB is being used as a component in a protective coating (where the MoB constitutes as much as 70% of the whole composition), which has outstanding durability against corrosion to molten light metals and/or their alloys (e.g., aluminum, zinc, and their alloys) [9].

Although electrochemical boriding of molybdenum had been studied in the past [3,21-22], the researchers used electrolytes mainly composed of alkali chlorides and alkali fluorides, which are known to be highly toxic to the environment at the time of operation due to the gaseous emissions generated at high temperatures. Malyshev et al. [22] synthesized molybdenum borides from the fluoride-based electrolyte by an electrochemical co-deposition process at 900°C. They obtained a mixture of Mo, $Mo_2B$, MoB, and $Mo_2B_5$ in 30 min, whereas they found single-phase $Mo_2B_5$ in 60 min. As a consequence of electrochemical boriding for 7 h at 950°C, Kuznetsov et al. [3] achieved a 48-μm-thick boride layer consisting of $Mo_2B$, MoB, and $Mo_2B_5$. One drawback in their study seems to have been the preparation of the electrolyte, which took many hours because of the additional steps of recrystallization of each component in the electrolyte and stabilization of the molten salt. In an earlier study conducted by Bonomi and co-workers [21], single-phase $Mo_2B_5$ was attained by varying time, temperature, and current density in the electrochemical

boriding method. In the present work we used an ultra-clean electrochemical boriding process (no greenhouse gas emissions) under a wide range of conditions to synthesize thick, hard, and homogeneous molybdenum boride phases in a very short duration. The only boride used in our experiments was naturally abundant borax ($Na_2B_4O_7$). We also proved that the use of relatively low process temperatures (down to 900°C) is sufficient to produce desired boride phases (i.e., boron-rich borides such as $Mo_2B_5$). This alone overcomes the necessity for using much higher temperatures (up to 1400°C), as in spark plasma sintering (SPS). For the same temperature and time, electrochemical boriding is found to produce much thicker layers than SPS.

## 2. Experimental

Molybdenum plates (99.5% purity) were initially ground and polished down to 1200 grit size using a series of SiC emery papers to remove the oxide layers and other contaminants from the surface. Prior to the boriding experiments, all samples were ultrasonically cleaned in acetone for 15 min. The equipment used in the electrochemical boriding experiments as well as the procedure was described in detail in our previous study [1]. The experiments were conducted at 900, 950, and 1000°C at a current density of 500 mA/cm$^2$. The process duration varied between 30 and 180 min.

After boriding, the samples were cut into pieces in cross section, cast in epoxy, and then ground and polished progressively in order to reveal and investigate the boride layers for their structural morphology by using an Olympus STM6 optical microscope. The phases formed during boriding were investigated with a thin-film diffractometer (Philips Xpert2) at regular 2θ-ω and glancing angle (1°) with Cu-Kα radiation and a wavelength of 1.54 Å. Micro-hardness measurements were performed with a Shimadzu HMV Micro Hardness Tester under a 50 g load. We also used Rockwell C equipment with 150 kg load to obtain information on the adhesion of the boride layers according to a protocol developed by Daimler-Benz.

## 3. Results and Discussion

### *3.1. Morphology and thickness of the boride layers*

Figure 1 shows an optical micrograph of the cross-sectional morphology of a borided Mo plate (1000°C, 2 h, and 500 mA/cm$^2$). The average thickness of the boride layer is around 47 µm. The contrast difference indicates that two different phases formed on the molybdenum substrate after boriding. The uppermost layer (with a gray or darker contrast) is ~35-µm thick and dense with a band-like morphology, while the layer beneath (white contrasting intermediate layer) is relatively thin (9 µm) and has a wavy morphology.

We performed a series of boriding experiments at different temperatures to explore the effect of temperature on boride phase formation and the thickness of the resultant boride layers at a current density of 500 mA/cm$^2$ for 60 min. The optical micrographs from the cross sections of each sample are shown in Fig. 2. An increment of 50°C in the process temperature resulted in a 10% increase in the thickness of the total boride layer (e.g., from 900°C to 950°C). The overall thicknesses of boride layers were 34–47 µm, and no cracking or delamination of the layer was observed. Kuznetsov et al. [3,13] reported that 16-µm and 48-µm thick boride layers could be achieved on molybdenum substrate after currentless and electrochemical boriding, respectively, at 950°C after 7 hours in alkaline chloride and fluoride-based molten salts. Both methods resulted in different boride phases: currentless boriding yielded a layer consisting of $Mo_2B$/MoB, while electrochemical boriding resulted in a multi-zone $Mo_2B$/MoB/$Mo_2B_5$ layers. These researchers also concluded that the $Mo_2B$/MoB layer failed to protect molybdenum from oxidation [3]. Based on the available literature data, the electrochemical boriding used in our study offered much

thicker boride layers (~47 μm) at the same process temperature (950°C) but at much shorter durations (about 2 h).

Figure 3 shows the relationship between the process duration and layer thickness as a function of boriding temperature. Each group of samples (i.e., the Mo plates were borided for 30 min at different temperatures but at constant current density of 500 mA/cm$^2$ ) reveals a linear fit; also shown are the $R^2$ values derived from the linear trends for the different process durations. The effect of temperature seems to be weak, although we used a lower temperature range as compared to other techniques (e.g., up to 1400°C for SPS [7]). Increasing process duration, however, seemed to have a pronounced effect on the layer growth. The boride layer almost doubled in thickness when the process duration was increased from 30 min to 60 min, and this growth rate started to slow down after 60 min. An example of the duration effect (1000°C and 500 mA/cm$^2$) is shown in Fig. 4. As is obvious from the graph, the boride layer growth slows down after 60 min, indicating that the boron diffusion decelerates as the layer thickness increases. As will be discussed later, this type of growth behavior strongly depends on the boron diffusion through the boride layer on top as well as the substrate material and should be investigated in detail by a kinetic approach.

*3.2. Kinetic study*

Regarding the diffusion of boron atoms from the surface into the substrate, the growth rate of the boride layer follows a parabolic trend according to the following equation [1,2]:

$$d^2 = Kt \tag{1}$$

where *d* is the thickness of the boride layer, *K* is the growth rate constant, and *t* is the duration for the boriding process. The growth rate constant (*K*) depends on the diffusion of boron and the temperature according to the Arrhenius equation [1,2]:

$$K = K_0 \, exp(\frac{-Q}{RT}) \tag{2}$$

where $K_0$ is pre-exponential constant, $Q$ is the activation energy, $T$ is the temperature, and $R$ is the universal gas constant. The parabolic relationship for the variation in boride layer thickness with respect to the different process temperatures is plotted in Fig. 5. As the process duration increases, the rate of boride formation on the substrate (at all given temperatures) slows down. In other words, the diffusion rate of boron atoms into the substrate (rate-controlling step [1-3]) decelerates even though there is a continuous boron reduction on the surface. The activation energy was calculated from the slope of ln ($K$) plotted versus $1/T$ (Fig. 6). The Q value was calculated to be 47.6 kJ/mol, which is far below the only literature value (218.8 kJ/mol) available for molybdenum [7]. We hypothesize that the number of boron atoms being reduced and saturated on the molybdenum surface is large, and this saturation is fast due to the electrochemical reaction. Later, boron atoms diffuse to the substrate until achieving the diffusion limit and form thick boride layers in a relatively short time as compared to the other boriding methods. This behavior may be the probable reason of the $Q$ value obtained in electrochemical boriding being lower than that found with the SPS method [7].

*3.3. X-ray diffraction (XRD) studies*

The XRD pattern scans (both glancing angle of 1° and regular $2\theta$-$\omega$) of borided Mo samples (at 900°C for 60 min at a current density of 500 mA/cm$^2$) are shown in Fig. 7. Figure 8 compares the resultant $2\theta$–d-spacings with the curve derived from the standard JCPDS (# 089-0336) file for $Mo_2B_{4.027}$ and shows an exact match. Also, the crystallographic characteristics of some molybdenum borides are also given in Table 1 to understand to the results obtained from XRD studies.

The thin-film XRD profile indicates that the top layer is a single phase of $Mo_2B_{4.027}$, which is the first time this has been reported. This phase is very hard but also brittle (as will be seen from the

Rockwell C adhesion tests below). The regular $2\theta$–$\omega$ scans of the same sample indicated that the main component through the inner layer is $Mo_2B_5$ phase with a similar XRD profile to $Mo_2B_{4.027}$.

Among the transition metal borides, Group VI metal borides (e.g., Mo, Cr, and W borides) in hexagonal crystal structure are reported to be unstable [25]. The Mo–B phase diagram (Fig. 9) shows three phases that are stable at room temperature: $Mo_2B$, α-MoB, and $Mo_2B_5$. The unstable hexagonal $MoB_2$ phase decomposes to α-MoB and $Mo_2B_5$ at around 1517°C upon cooling. Our XRD studies did not show any traces of $Mo_2B$ or α-MoB, but $Mo_2B_{4.027}$ and $Mo_2B_5$ were found to be the dominant phases for the top and inner layers, respectively. Due to their smaller atom size, boron atoms seem to diffuse easily through the molybdenum substrate, in which the diffusivity of boron atoms in the boron-rich borides is greater than that for metal-rich borides. The $Mo_2B$ and MoB phases are known to form if the boron source supplied on the surface is limited, whereas $Mo_2B_5$ formation requires a large supply of boron atoms [17]. The latter is the most probable scenario in our case, and continuous boron atom deposition on the surface results in mainly boron-rich phases. Also note that high cathodic current density is required for the formation of $Mo_2B_5$ phase, as reported elsewhere [3]. Overall, boron-rich borides (e.g., $Mo_2B_5$) are the most desirable as a protective coating in high temperature applications (up to 1600°C [8]).

*3.4. Vickers hardness and Rockwell C adhesion tests*

A Vickers micro-hardness machine was used to measure the hardness of the boride layers at a load of 50 g. The hardness profile and hardness values belonging to each region are shown in Fig. 10 and Table 2, respectively. The uppermost layer ($Mo_2B_{4.027}$) has hardness values of about 3150 ± 100 HV. There seems to be a transition region between the boride layers, which have a lower hardness value than the top layer. For the inner boride layer, where $Mo_2B_5$ is present, the maximum hardness value was measured to be 1960 HV.

To assess the adhesion characteristics of the boride layers formed on molybdenum, we conducted Rockwell C indentation tests according to the Daimler-Benz protocol. The resultant micrograph is shown in Fig. 11. As is obvious, on the indented surface, the adhesion of the coating is average, since there is a crack network with delamination evident on the surface. Based on the Daimler-Benz adhesion chart, the adhesion of the boride layers is eligible for the HF3 category, which is considered to be normal adhesion.

## 4. Conclusions

Electrochemical boriding has been performed to more rapidly produce super-hard molybdenum boride layers on a substrate. The present process produces a 38-μm-thick boride layer in 60 min, as opposed to 7 h needed to produce a 16-μm-thick layer by currentless boriding. In other words, the resultant layer is 2.5 times the thickness in $1/7^{th}$ the time. Optical micrographs show that the boride layers are dense and homogeneous, consisting of two regions (by virtue of the contrast). The outer boride layer is composed of a single phase, $Mo_2B_{4.027}$; varies in thickness between 20 and 37 μm; and is very hard (i.e., max. 3250 HV). The bottom layer is composed of sub-stoichiometric $Mo_2B_5$ phase, and it provides a transition zone from the top boride layer to the un-borided Mo matrix. The activation energy was calculated to be 47.6 kJ/mol, which is substantially below the available literature value of 218.8 kJ/mol [7]. The XRD studies showed that $Mo_2B_{4.027}$ phase was the most predominant within the top layer, which also offers very high hardness. The boride layer thickness increased with increasing process duration from ~22 to ~48 μm for the same boriding temperature (i.e., 1000° C). The Rockwell C adhesion tests verified normal adhesion for the boride layers.. Future work will examine forming a single boride phase on molybdenum and improving the coating adhesion.

## Acknowledgments

The authors would like to thank the U.S. Department of Energy, Office of Energy Efficiency and Renewable Energy, ITP, under Contract Number DE-AC02-06CH11357 with the U.S. Department of Energy for supporting this work. They would also like to thank for the X-ray diffraction study, which was carried out in the Materials Characterization Laboratory, Istanbul Technical University. The authors would like to thank Gerald Jeka for doing the microscopy imaging and helping in sample preparation.

**References**


1. O. Kahvecioglu, V. Sista, O.L. Eryilmaz, A. Erdemir, S. Timur, Thin Solid Films 520 (5) (2011) 1575–1581.
2. V. Sista, O. Kahvecioglu, O.L. Eryilmaz, A. Erdemir, S. Timur, Thin Solid Films 520 (5) (2011) 1582–1588.
3. S.A. Kuznetsov, S.V. Kuznetsova, E.V. Rebrov, M.J.M. Mies, M.H.J.M. de Croon, J.C. Schouten, Surf. Coat. Tech. 195 (2005) 182-188.
4. K. Kudaka, K. Iizumi, T. Sasaki, S. Okada, J. Alloys Compd. 315 (2001) 104-107.
5. Y. Li, Y. Fan, Y. Chen, J. Solid State Chem. 170 (2003) 135-141.
6. G. Yang, H. Z-kun, X. Xiaolei, X. Gang, J. Thermal Spray Tech. 10 (3) (2001) 456-460.
7. L.G. Yu, K.A. Khor, G. Sundararajan, Surf. Coat. Tech. 201 (2006) 2849-2853.
8. R. Steinitz, I. Binder, D. Moskowitz, J. Metals, Sept. 1952, 983-987.
9. T. Yasuda, A. Banno, T. Ito, K. Kiyoshi, K. Ishibayashi, US Patent No. 6,238,807 B1, May 29, 2001.
10. T. Kudo, H. Obayashi, US Patent No. 4,242,421, Dec 30, 1980.
11. I. R. Shein, A.L. Ivanovskii, Phys. Rev. B 73 (2006) 144108/1-9.
12. L.N. Kugai, Poroshkovaya Metallurgiya 12 (108) (1971) 54-57.
13. S.A. Kuznetsov, E.V. Rebrov, M.J.M. Mies, M.H.J.M. de Croon, J. C. Schouten, Surf. Coat. Tech. 201 (2006) 971-978.
14. A. Koutsomichalis, H. Badekas, Scripta Metal. Mater. 29 (8) (1993) 1125-1129.
15. V.V. Malyshev, A. Gab, M. Gaune-Escard, Mater. Manufact. Processes 23 (2008) 748-751.

16. M.V. Babu, R.K. Kumar, O. Prabhakar, N. G. Shankar, Surf. Coat. Tech. 79 (1-3) (1996) 276-288.

17. J. Brandstötter, W. Lengauer, J. Alloys Compd. 262-263 (1997) 390-396.

18. C.L. Yeh, W.S. Hsu, J. Alloys Compd. 457 (2008) 191-197.

19. H. Klesnar, T.L. Aselage, B. Morosin, G.H. Kwei, A.C. Lawson, J. Alloys Compd. 241 (1996) 180-186.

20. H.E. Camurlu, J. Alloys Compd. 509 (2011) 5431-5436.

21. A. Bonomi, H. Giess, C. Gentaz, Electrodep. Surf. Treat. 1 (1972/1973) 419-427.

22. V.V. Malyshev, A. Gab, D. Shakhnin, A.M. Popescu, V. Constantin, M. Olteanu, Academia Romana 55 (4) (2010) 233-238.

23. A.C. Silva, M.J. Kaufmann, Intermetallics 5 (1997) 1-15.

24. L. Vines, J. Cain, S. Koegnigseder, F. Fujishiro, US Patent No. 5,329,161, Jul. 12, 1994.

25. A.L. Ivanovskii, I.R. Shein, N.I. Medvedeva, Russian Chem. Rev. 77 (5) (2008) 467-486.

26. P. Rogl and J. C. Schuster, Phase Diagrams of Ternary Boron Nitride and Silicon Nitride Systems, Monograph Series on Alloy Phase Diagrams, ASM International, Materials Park, Ohio, 1992, pp. 64-67.

27. T. Watanabe, S. Kono, US Patent No. 4,379,852, Apr. 12, 1983.

28. V.N. Gurin, L.I. Derkachenko, A.I. Shelykh, Refract. Ind. Ceram. 48 (4) (2007), 247-252.

## List of Figures

Figure 1. General morphology of boride layers obtained at 1000°C for 2 h at a current density of 500 mA/cm$^2$.

Figure 2. Cross-sectional images of the samples borided at a) 900°C, (b) 950°C, and (c) 1000°C for 60 min at a current density of 500 mA/cm$^2$.

Figure 3. Thickness variation with temperature as a function of process duration.

Figure 4. Variation of total boride layer thickness with process duration (samples borided at 1000°C and 500 mA/cm$^2$).

Figure 5. Variation of total boride layer thickness with time at different temperatures.

Figure 6. Variation of ln ($K$) vs. $1/T$ for activation energy calculation.

Figure 7. XRD profiles of the Mo sample after electrochemical treatment (60 min, 900°C, and 500 mA/cm$^2$): (a) glancing angle (1°) and (b) regular $2\theta$-$\omega$ scans of borided layer.

Figure 8. Comparison of experimental and literature 2θ-d spacing plots of the glancing angle scan.

Figure 9. Mo–B binary phase diagram [26].

Figure 10. Cross-sectional image of micro-indentation marks at a load of 50 g (900°C, 2 h, 500 mA/cm$^2$).

Figure 11. Rockwell C adhesion test (950°C, 2 hr, 500 mA/cm$^2$).

**Figure 1**

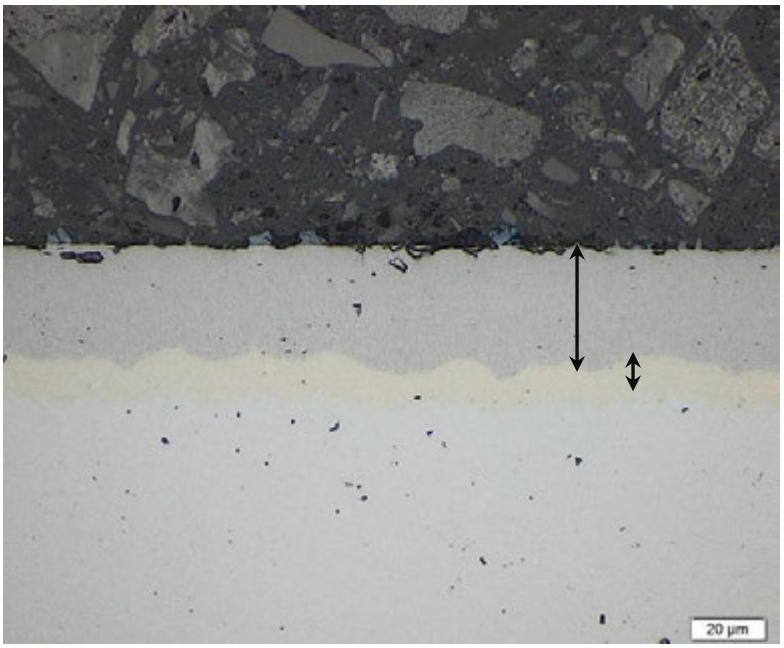


Figure 1

**Figure 2**

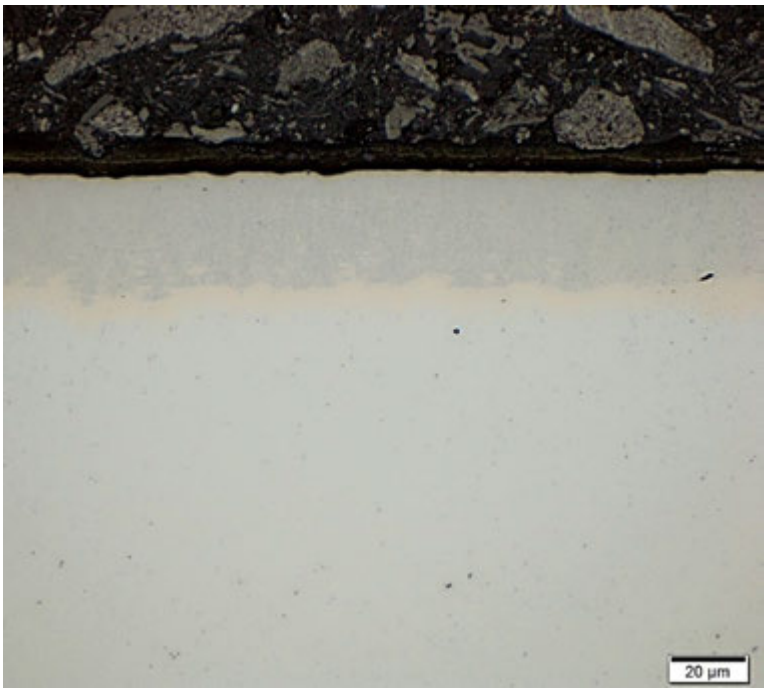


(a)

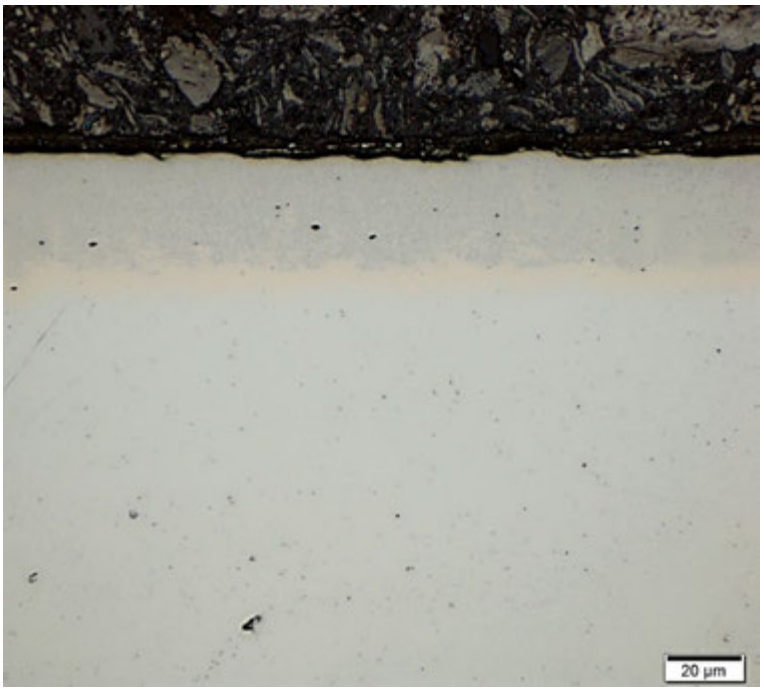


(b)

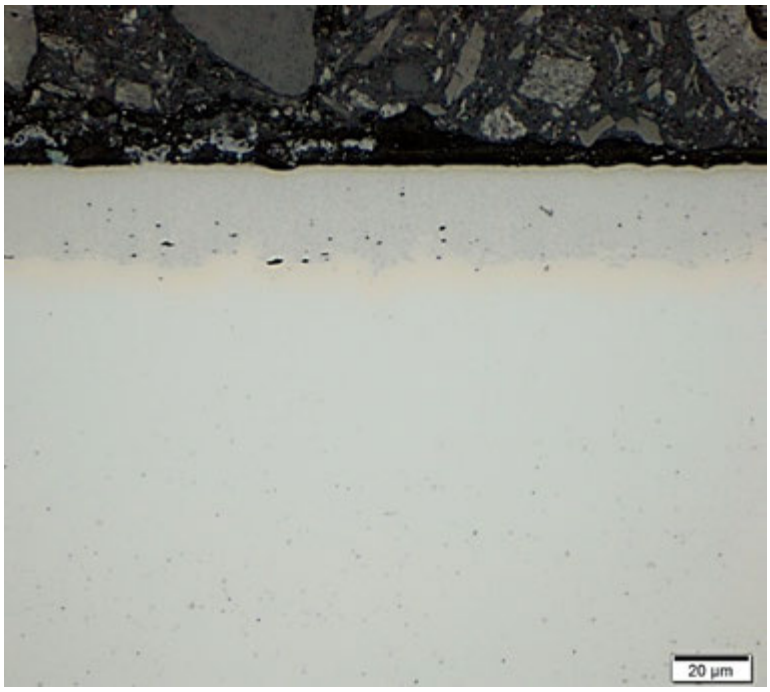


(c)

Figure 2

**Figure 3**

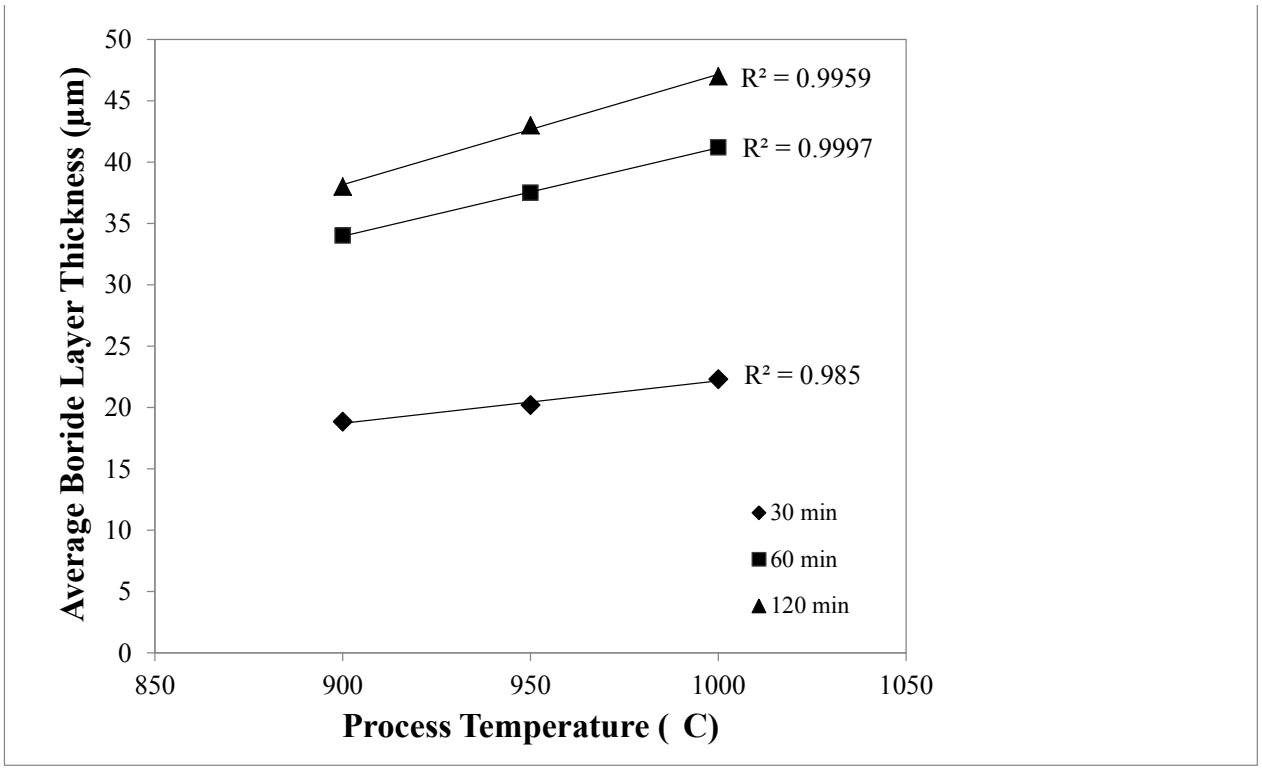


Figure 3

**Figure 4**

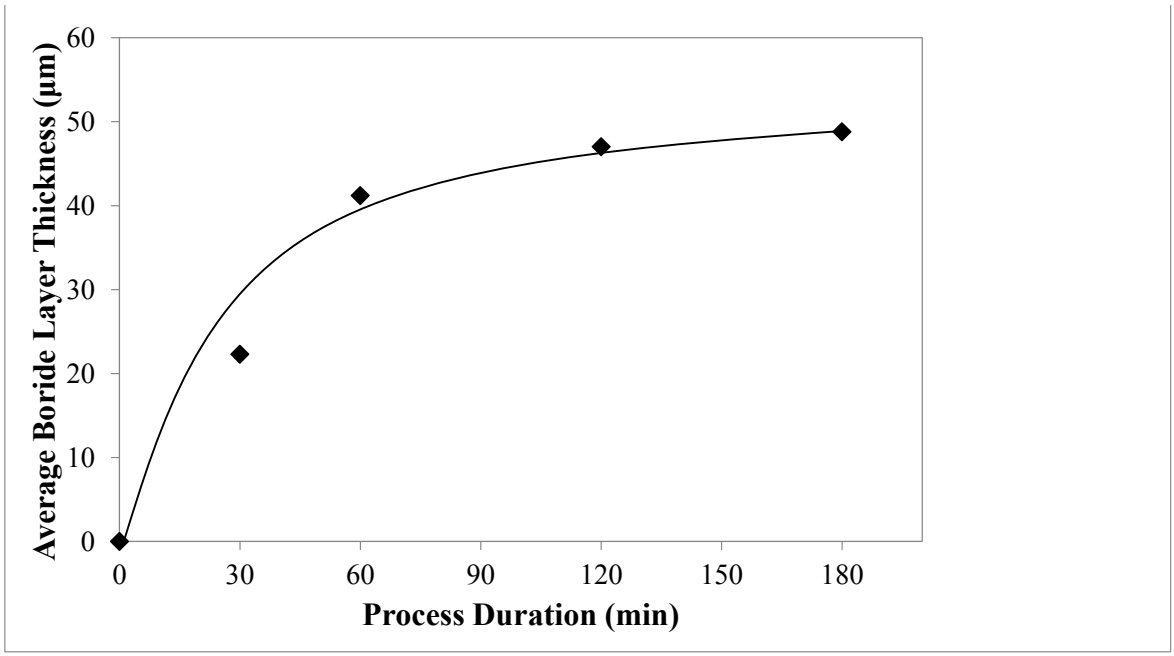


Figure 4

**Figure 5**

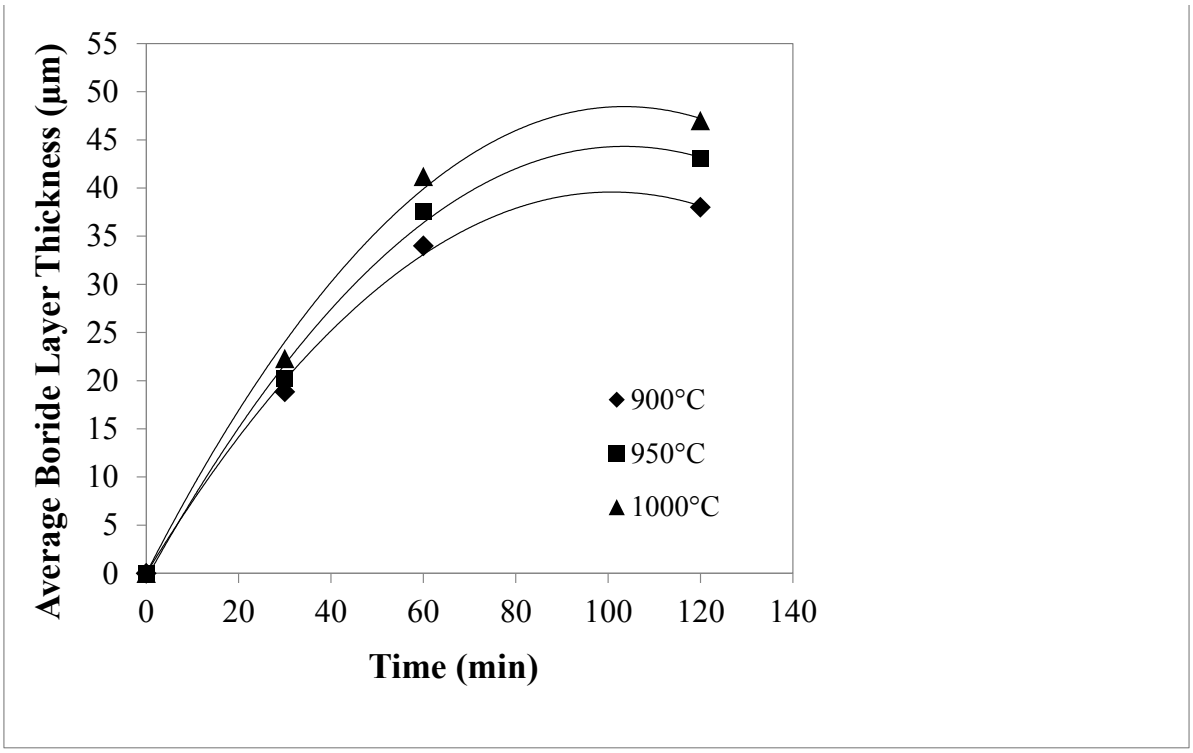


Figure 5

**Figure 6**

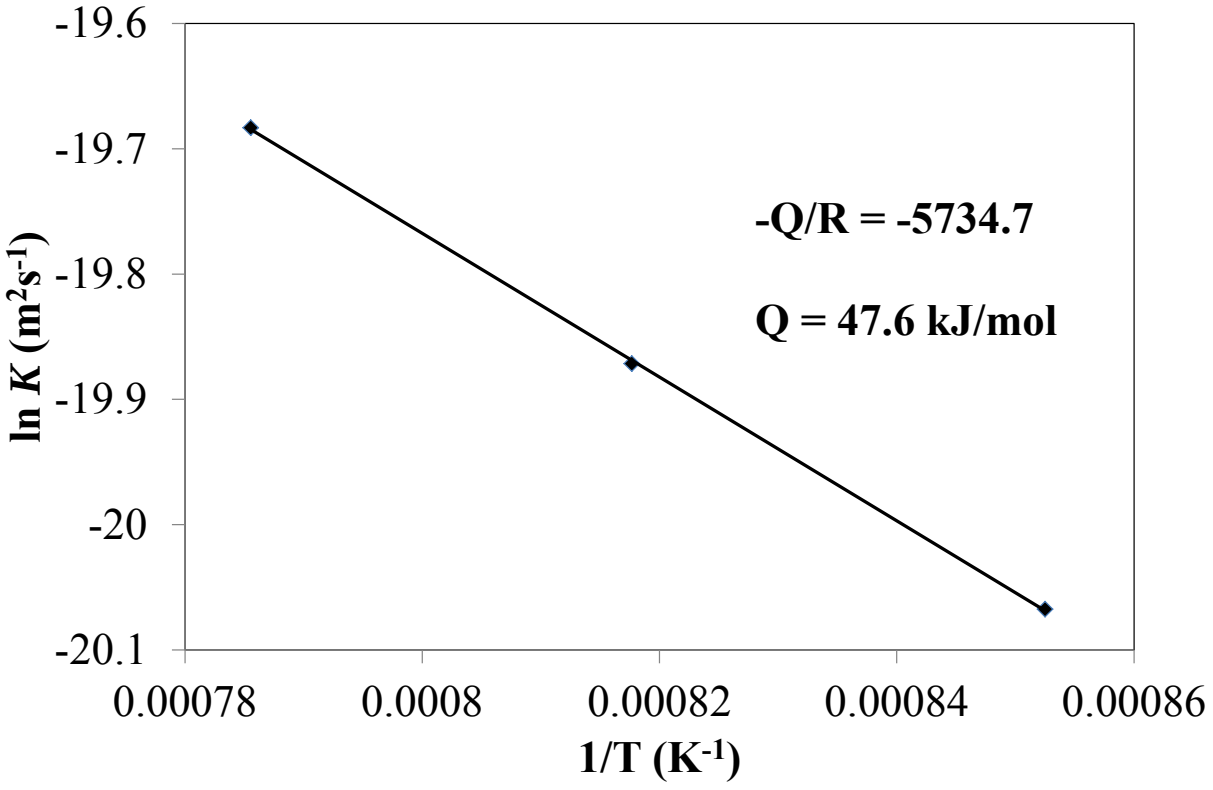


Figure 6

**Figure 7**

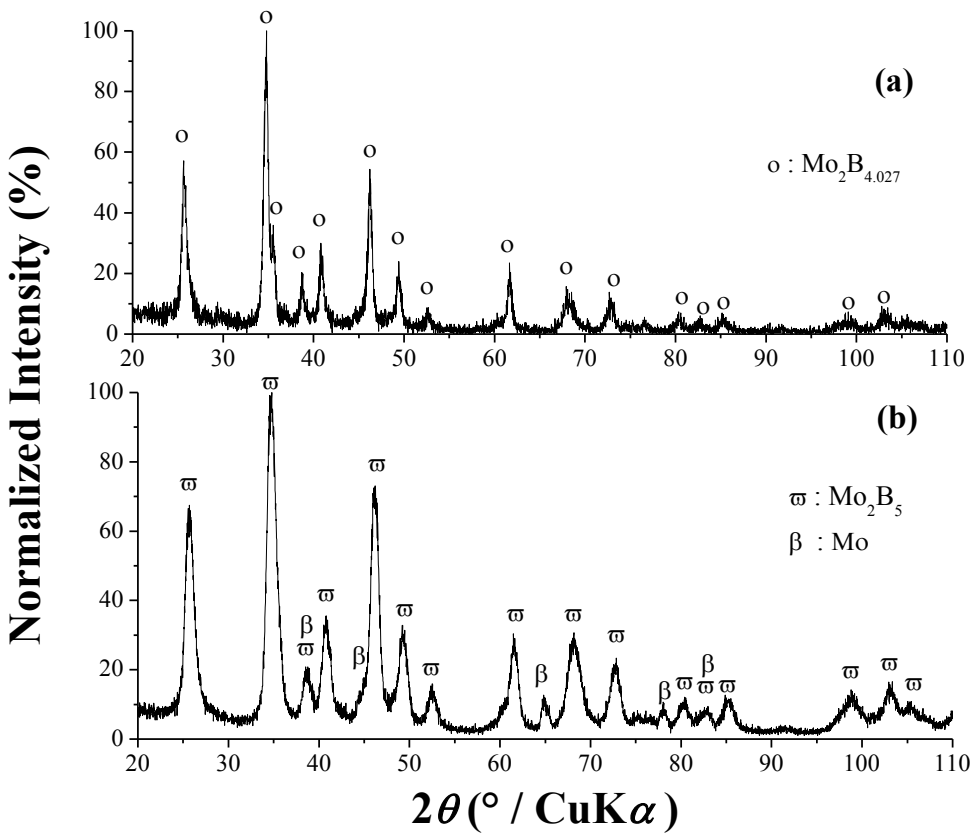


Figure 7

**Figure 8**

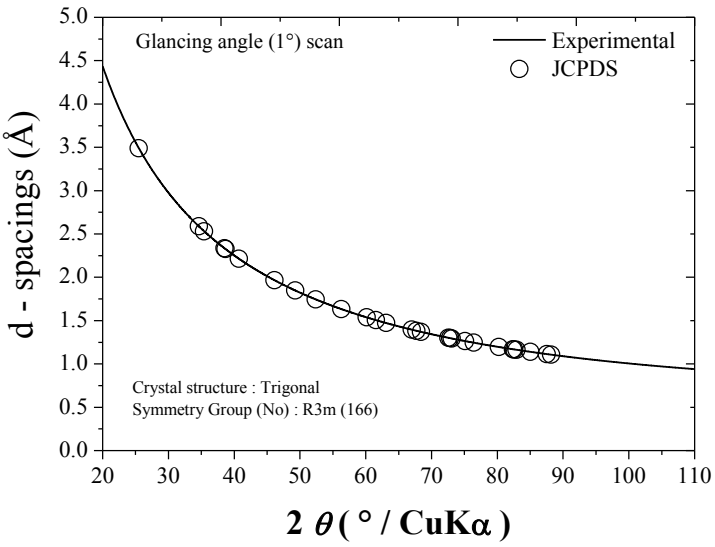


Figure 8

**Figure 9**

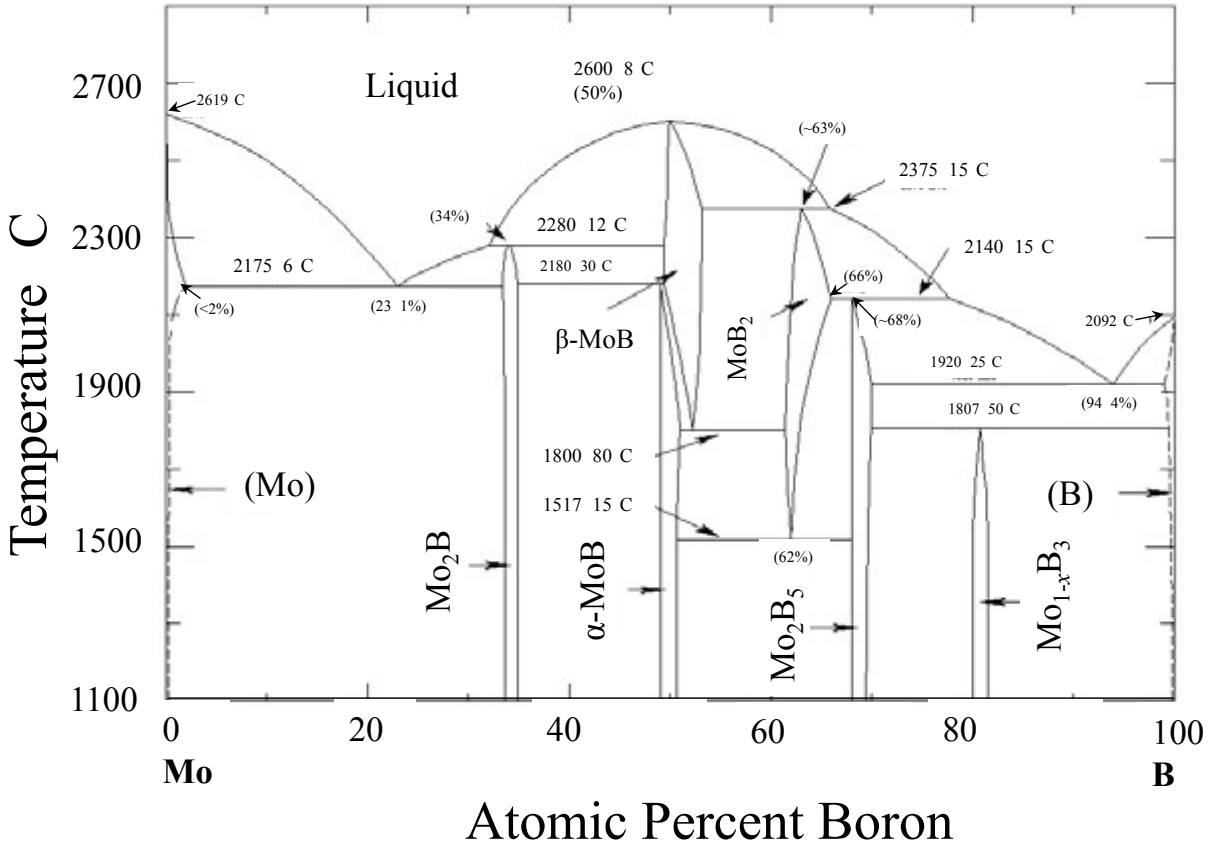


Figure 9

**Figure 10**

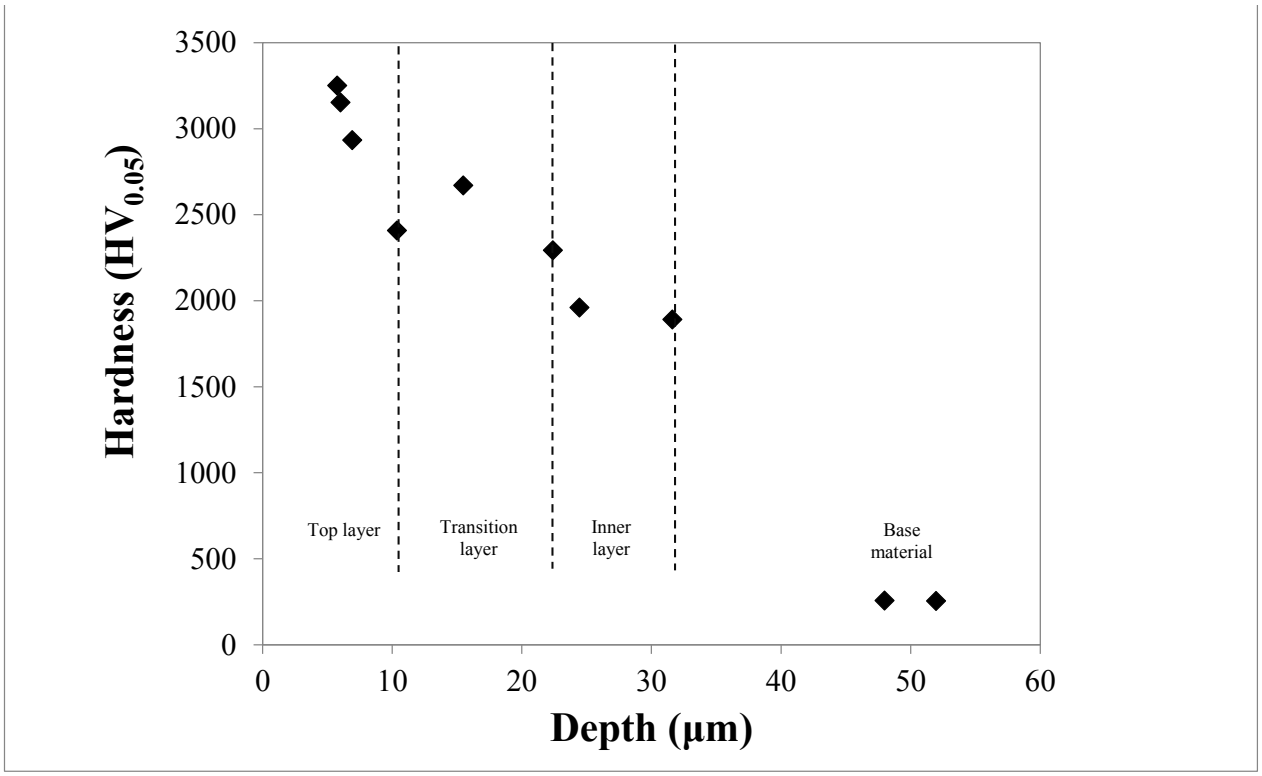


Figure 10

**Figure 11**

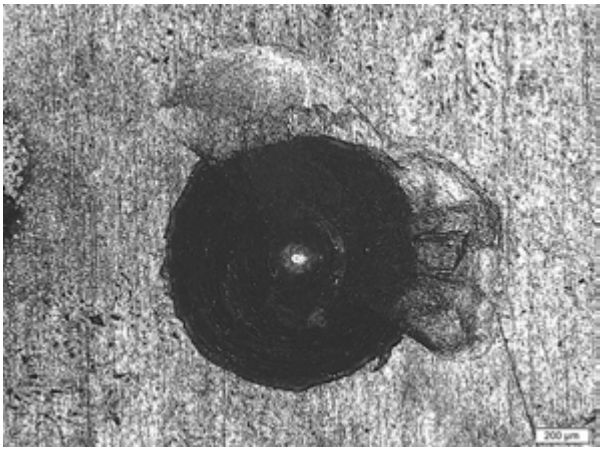


Figure 11

**Table 1**

Table 1. Crystallographic parameters of some molybdenum borides

| ***Phase*** | $Mo_2B_{4.027}$ #089-0336 | $Mo_2B_5$ #038-1460 | $Mo_2B_4$ #077-0807 | $MoB_2$ #073-0704 | $MoB_{2.5}$ #073-1770 |
|---|---|---|---|---|---|
| Crystal structure | Rhombohedral | Rhombohedral | Rhombohedral | Rhombohedral | Rhombohedral |
| Space Group | R m | R m | R m | R m | R m |
| Volume, $Å^3$ | 164.45 | 164.47 | 164.69 | 165.11 | 164.33 |
| Lattice Parameters, Å | $a$ = 3.0116<br>$c$ = 20.9370 | $a$ = 3.0117<br>$c$ = 20.9369 | $a$ = 3.0136<br>$c$ = 20.9390 | $a$ = 3.0152<br>$c$ = 20.9710 | $a$ = 3.011<br>$c$ = 20.9300 |
| $2\theta$ (101) | 34.631 | 34.622 | 34.607 | 34.588 | 34.638 |
| $2\theta$ (006) | 25.506 | 25.503 | 25.503 | 25.464 | 25.515 |
| $2\theta$ (107) | 46.141 | 46.134 | 46.121 | 46.074 | 46.154 |
| $d_{(101)}$, Å | 2.58812 | 2.58873 | 2.58981 | 2.59123 | 2.58760 |
| $d_{(006)}$, Å | 3.48950 | 3.48989 | 3.48983 | 3.49517 | 3.48833 |
| $d_{(107)}$, Å | 1.96574 | 1.96602 | 1.96656 | 1.96845 | 1.96523 |

* JCPDS Card Number

**Table 2**

Table 2. Vickers micro-hardness values of the regions

| ***Region*** | $Mo_2B_{4.027}$ | Transition Zone | $Mo_2B_5$ | Mo substrate |
|---|---|---|---|---|
| $HV_{0.05}$ | 3150±100 | 2670±270 | 1920±40 | 255±1 |
| Ref. [8] | N/A | N/A | 2350** | N/A |
| Ref. [21] | N/A | N/A | 3000* | N/A |
| Ref. [27] | N/A | N/A | 3000 | N/A |
| Ref. [28] | N/A | N/A | 2500±300*** | N/A |

* 100 g of load on the cross section.
** 50 g of load on the cross section.
*** Single crystal.